Chaos, Solitons and Fractals 165 (2022) 112775

Contents lists available at ScienceDirect

Chaos, Solitons and Fractals

journal homepage: www.elsevier.com/locate/chaos

Fronts connecting stripe patterns with a uniform state: Zigzag coarsening dynamics, and pinning effect

Marcel G. Clerc [a], Daniel Escaff [b,*], René G. Rojas [c]

[a] Departamento de Física and Millennium Institute for Research in Optics, FCFM, Universidad de Chile, Casilla 487-3, Santiago, Chile
[b] Universidad de los Andes, Chile. Monseñor Alvaro del Portillo 12455, Las Condes, Santiago, Chile
[c] Instituto de Física, Pontificia Universidad Católica de Valparaíso, Casilla 4059, Valparaíso, Chile

ARTICLE INFO

Keywords:
Pattern formation

ABSTRACT

The propagation of interfaces between different equilibria exhibits a rich dynamics and morphology, where stalactites and snowflakes are paradigmatic examples. Here, we study the stability features of flat fronts within the framework of the subcritical Newell–Whitehead–Segel equation. This universal amplitude equation accounts for stripe formation near a weakly inverted bifurcation and front solutions between a uniform state and a stripes pattern. We show that these domain walls are linearly unstable. The flat interface develops a transversal pattern-like structure with a well defined wavelength, later on, the transversal structure becomes a zigzag structure: This zigzag displays a coarsening dynamics, with the consequent growing of the wavelength. We study the relation between this interface instability and those exhibited by the interface connecting a stripes pattern with a uniform state in the theoretical framework of subcritical Swift–Hohenberg equation. A transversally flat wall domain could be stabilized by the pinning effect, this dynamical behavior is lost in the subcritical Newell–Whitehead–Segel approach. However, this flat interface is a metastable state and in the presence of noise the system develops a similar behavior to the subcritical Newell–Whitehead–Segel equation.

1. Introduction

Non equilibrium processes often lead in nature to pattern formation developing from a uniform state through a spontaneous symmetry-breaking instability [1]. In the last decades, a lot of attention has been devoted to the study of pattern formation (see reviews [2–7] and the references therein) arising in systems such as chemical reactions, gas discharge systems, CO_2 lasers, liquid crystals, hydrodynamic or electroconvective instabilities and granular matter, to mention a few. A unified attempt to describe the dynamics of spatially periodic structures developed at the onset of spatial bifurcation is achieved by means of amplitude equations for critical modes [1]. Such a description is valid in the case of weak nonlinearities and for a slow spatial and temporal modulation of the base pattern [2,7]. As an example, the Newell–Whitehead–Segel equation describes the dynamics of a stripes pattern formed in two-dimensional isotropic systems [8].

Another ubiquitous phenomenon in nature is the interface dynamics or fronts propagation or domain walls dynamics [7]. The concept of front propagation, emerged in the field of population dynamics [9], has gained growing interest in biology [10], chemistry [11], physics [2,12], optics [13–16], and mathematics [17]. These interfaces connect two extended states, such as uniform states, periodic cellular patterns, uniform oscillations, standing waves, spatiotemporal chaotic states, and so forth. In one-dimensional systems, when one has an interface connecting two uniform stable states [16], the most favorable state (for instance, energetically) invades the other one with a constant speed. This speed is zero, that is the front is motionless, for a single value of the system parameters, which is well-known as the *Maxwell point* [18]. The above picture changes drastically when one considers an interface connecting a periodic cellular pattern state with a uniform one (or two different periodic patterns). Due to the breaking of the spatial translation symmetry, the interface is motionless in a range of parameters, *the pinning range* [18–22]. Even if one of the extended states is more favorable (in an energetically sense, for example), the front remains at rest. Experimentally, the pinning–depinning transition of fronts between pattern states was characterized based on a liquid crystal light valve with optical feedback [23]. However, this pinning effect is missed in the amplitude equations approach to the patterns forming processes [18]. The reason for that is related with the request of weak nonlinearities. Namely, if the nonlinearities scale with the bifurcation parameter ε ($0 < \varepsilon \ll 1$), the amplitude equations method assumes that one can expand the system variables in a power series of ε or $\varepsilon^{1/m}$ (m is an integer). The asymptotic amplitude equations itself

* Corresponding author.
E-mail address: descaff@miuandes.cl (D. Escaff).

https://doi.org/10.1016/j.chaos.2022.112775
Received 19 July 2022; Received in revised form 11 September 2022; Accepted 1 October 2022
Available online 21 October 2022

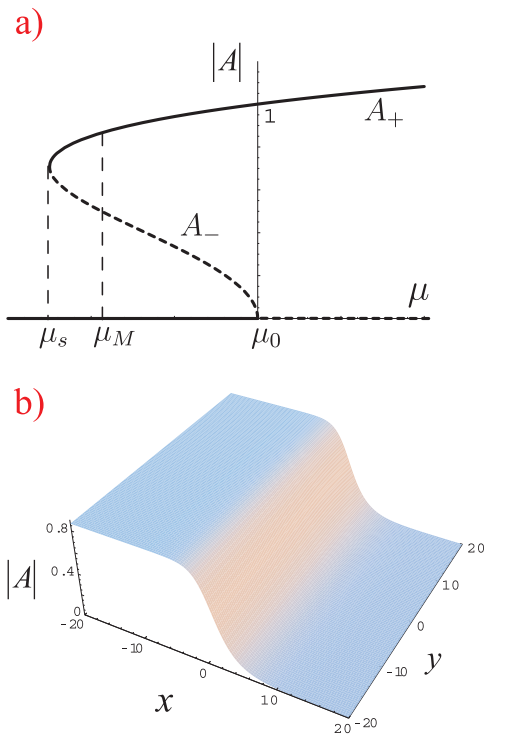

Fig. 1. (a) Bifurcation diagram of the uniform solutions of model (1), the solid and dashed lines stand for stable and unstable solutions, respectively. (b) Front solution (2), A_F^+ with $P = \theta = 0$.

is the lowest order in this expansion, that is, the dominate dynamic. Nevertheless, it has been shown that the pinning range is exponentially small in this scaling, i.e. scales as $\exp(-\varepsilon^{-n})$ with $n > 0$ [24]. Then, the pinning phenomenon is missed in all the orders of the expansion. A notorious effort, to correct it, has been performed via amended amplitude equations [25,26].

In bidimensional dynamical systems, flat fronts connecting patterns and uniform states have an extra degree of freedom, the transversal direction. In the case of a front that links stripes pattern with a uniform state, it has been shown that a very rich transversal dynamics could emerge [27–32]. For example, a depinning process has been reported in context of the supercritical Swift–Hohenberg equation, which is related to a transversal instability that leads to the formation of a labyrinth pattern [27]. In the case of subcritical Swift–Hohenberg model a quite rich variety of pattern-like transversal structures have been reported [28–31]. In this context, it has been also suggested the possibility of a zigzag coarsening process [29], this phenomenon with be discussed in detail in this work. Furthermore, beyond the prototypical Swift–Hohenberg model, this kind of phenomena seem to be relevant in several pattern-forming processes, such as vibrated granular layers [33], copolymer thin films [34], molecular electronics [35,36], convectons in the context of fluid dynamics [37–39], or vegetation population dynamics in semiarid zones [40,41], where the instability of circularly shaped interfaces allow the repopulation of territories devoid of vegetation due to a self-replication of the biomass (for front dynamics and self-replication in population dynamics, it might be also seen Refs. [42–48]). Moreover, nonlinear optics has been another fruitful field to study front dynamics [49], where, for instance, fingering instabilities in flat and circularly shaped interfaces are well documented [50–52]. At this point, it might sound pertinent to pay more attention to universal descriptions of pattern formation, such as amplitude equations.

The aim of this work is to study interface dynamics in the framework of subcritical Newell–Whitehead–Segel equation. In particular, we analyze the dynamics of a flat interface and show that these fronts are linearly unstable; that is, after an infinitesimal perturbation the flat configuration, the interface initially develops a transversal pattern-like structure with a well-defined wavelength; later on, the transversal structure becomes a zigzag structure, which displays a coarsening dynamics. Then, we study the relationship between this interface instability and those exhibited by the interface connecting a stripe pattern with a uniform state in the framework of the subcritical Swift–Hohenberg equation. The model and the front solution at the Maxwell point are presented in Section 2. In Section 3, it is shown that this front is linearly unstable. In Section 4, we study the nonlinear regime, where the interface becomes a zigzag structure which displays a coarsening process. In Section 5, we analyze the phenomenology exhibited by the domain wall out of the Maxwell point. As we mentioned above, since amplitude equations fail in describing the pinning effect, its utility for the study of fronts involving spatially periodic structures might be questionable. The pertinence between these results and the description of pattern formation out of equilibrium is discussed is Section 6. In connection with our previous work on the quintic Swift–Hohenberg equation [29], it is shown that the pinning effect is able to stabilize a transversally flat interface between stripes and a uniform state (at least for the parameters reported in this work). However, it is a metastable state, in presence of noise the system exhibits the same dynamical behavior that the amplitude equation, namely, the formation of a zigzag structure which displays a coarsening dynamics. In Section 7, we present the conclusion and final remarks.

2. Subcritical Newell–Whitehead–Segel equation

Let us introduce the subcritical Newell–Whitehead–Segel equation [8] (subcritical-NWS)

$$\partial_t A = \mu A + |A|^2 A - |A|^4 A + \left(\partial_x - i\partial_{yy}\right)^2 A, \tag{1}$$

where $A(x, y, t)$ is a complex field, which accounts for the envelope of the stripes pattern, and μ is the bifurcation parameter which is a real free parameter. The sign of the cubic and quintic nonlinearities have been chosen in order to have a subcritical bifurcation at $\mu = 0$. The nonlinear and spatial coefficients have been normalized to one by appropriately scaling the amplitude, time, and space. The $\{x, y\}$ are the slow spatial variables that stand for the orthogonal and the transversal directions with respect to stripes pattern. The asymmetrical dependence of spatial derivatives is a consequence of the fact that the original pattern breaks the isotropy symmetry. The afore dynamical system has the Lyapunov functional,

$$\mathcal{F}\left[A, A^*\right] = \int \left\{ \left| \left(\partial_x - i\partial_{yy}\right) A \right|^2 + U\left(|A|\right) \right\} dxdy,$$

where

$$U\left(|A|\right) = \left(\frac{1}{3}|A|^4 - \frac{1}{2}|A|^2 - \mu \right) |A|^2 .$$

Therefore, the temporal evolution of amplitude Eq. (1) minimizes this functional ($d\mathcal{F}[A, A^*]/dt \leq 0$, during the system evolution).

The envelope Eq. (1) models the spatiotemporal evolution of the amplitude of stripes that are orthogonal to the x-direction, more precisely, a pattern with a profile $\mathrm{Re}\left[Ae^{iqx}\right]$, where q is the wavenumber of the pattern. Notice q has been removed from Eq. (1) by a spatial rescale. Hence, the nonzero uniform states of Eq. (1) represent spatially extended stripes. While, the trivial solution $A = 0$ represents a genuine uniform state. This trivial state $A = 0$ is stable when $\mu < 0$ and unstable when $\mu \geq 0$. Besides, the system has the nonzero amplitude solutions

$$A_\pm = \sqrt{\frac{1}{2}\left(1 \pm \sqrt{1 + 4\mu}\right)} e^{i\theta},$$

with θ an arbitrary constant, due to the translational invariance of the original pattern forming system. These nonzero solutions appear by saddle–node bifurcation at $\mu_s \equiv -1/4$, A_- is an unstable state and merges with $A = 0$ at $\mu = \mu_0 \equiv 0$, while A_+ remains stable for all

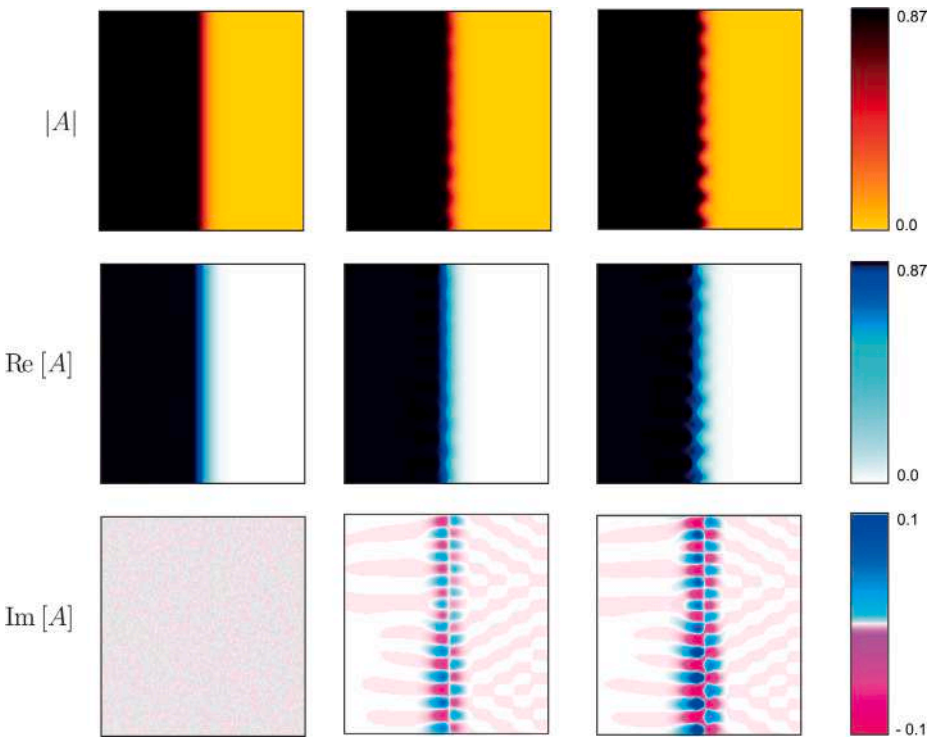

Fig. 2. Density plots of $|A|$ (up), $\mathrm{Re}\,[A]$ (middle) and $\mathrm{Im}\,[A]$ (down) of the model Eq. (1). The horizontal and vertical direction corresponds to x ($x \in [0, 199]$) and y ($y \in [0, 199]$) coordinate, respectively. Time grows up from left to right, the first states corresponds to $t = 0$ (the initial condition), the second one to $t = 3300$ and the last one to $t = 3800$.

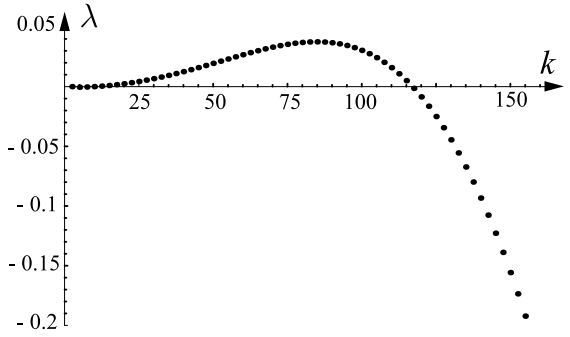

Fig. 3. Numerical computation of the $\lambda(k)$-spectrum (growth rate) as a function of wavenumber k.

$\mu > \mu_s$. Fig. 1(a) shows the bifurcation diagram of the uniform states of the subcritical-NWS equation. Therefore, a stable nonzero (pattern) coexists with a zero amplitude state (uniform state) within the range $\mu_s < \mu < \mu_0$, that is, in this region of parameters the system exhibits bistability.

We are interested to find a flat interface between these states, that is, to reach a domain wall parallel to the orientation of stripes. For the model Eq. (1), such spatial connection is motionless only at the Maxwell point $\mu = \mu_M \equiv -3/16$, and has the form

$$A_F^{\pm}(x) = \sqrt{\frac{3/4}{1 + e^{\pm\sqrt{3}(x-P)/2}}}\, e^{i\theta}, \tag{2}$$

where θ and P are arbitrary constants. The shape of this interface is shown in Fig. 1(b). Both, θ and P, are independent free parameters of the solution (2), that are related with the translational invariance of the underline pattern forming system. The parameter P is related with translation of the pattern envelop, while θ is related with the phase invariance, i.e. translation of the spatial oscillations.

3. Linear stability of a transversally flat interface

To investigate the stability of the front solution (2), we have performed numerical simulations of the model (1), using a finite difference method and a fourth order Runge–Kutta method for the time evolution. Furthermore, we have considered null flux boundary conditions in the x-direction and periodic boundary condition in the y-direction, in all the numerical simulations of the model Eq. (1).

We have taken as initial condition the front solution (2) with $\theta = 0$, i.e. a real field (without lost of generality due to the phase invariance), with a small stochastic perturbation. If the front (2) is stable, we expect that the initial condition evolves to a flat front, with a little translation of the free parameters of the non perturbed flat interface, that is, $\theta \to \theta + \delta\theta$ and $P \to P + \delta P$. However, independent of the smallness of the initial noisy perturbation, we have observed that the imaginary part of A increases systematically at the interface when time evolves. It is worthy to note that the imaginary part of A is a measure of the phase dynamics.

Fig. 2 shows the destabilization process; note that, the phase excitation occurs around a well defined wavelength (modulated by a long wavelength). As the excitation develops, the front position begins to move in a longitudinal inhomogeneous way, inducing the formation of a transversal structure with the same well-defined wavelength. The amplitude of this pattern-like structure grows at the early time of the system evolution.

To grasp the behavior of the longest transversal wavelength of the instability, we perform the following analysis: we prepare an initial condition from the front solution (2), promoting its position to a function of y coordinate, i.e. $P \to P(y) = P_0 + \delta P(y)$, where $\delta P(y)$ is a small profile with Gaussian shape. Then, the system is allowed to evolve for a short time, during this evolution we measure the front position $P(y, t)$, and its Fourier transform $\hat{P}_k(t)$. If the time of evolution is short enough, then the system stays in the *linear regime*, which is defined by the criterion

$$\hat{P}_k(t) \cong \hat{P}_k(0) \exp[\lambda(k)\, t],$$

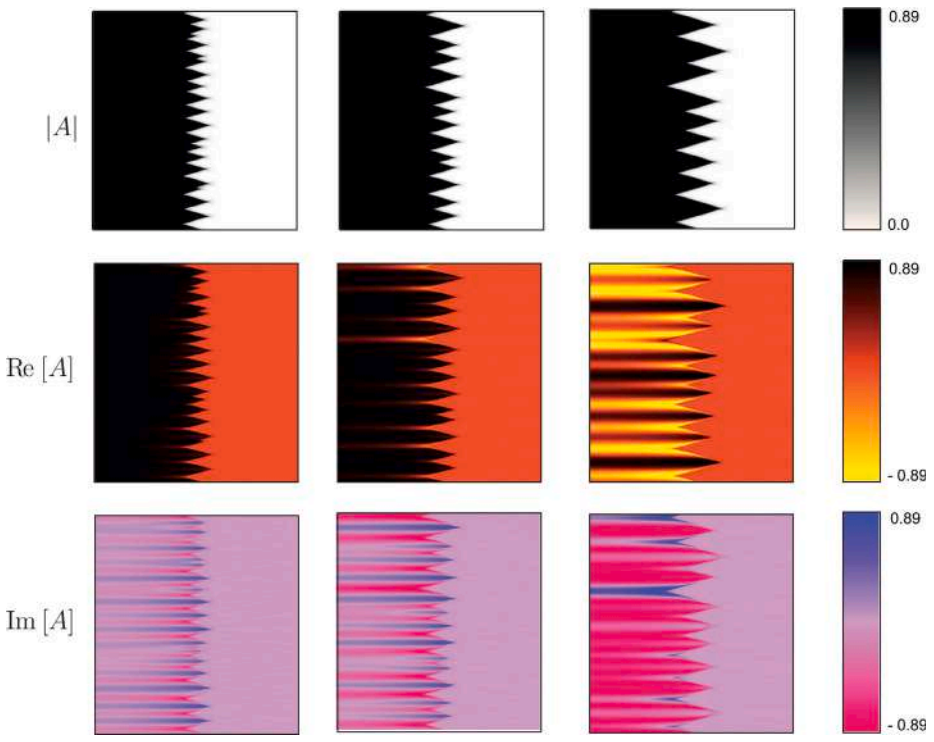

Fig. 4. Density plots of $|A|$ (up), $\mathrm{Re}\,[A]$ (middle) and $\mathrm{Im}\,[A]$ (down) of the model Eq. (1). The horizontal direction corresponds to x ($x \in [4400, 5000]$, and the simulation has been performed in the domain $x \in [0, 9999]$) and the vertical one to y ($y \in [0, 200]$, and the simulation has been performed in the domain $y \in [0, 299]$). Time grows up from left to right, if the initial condition correspond to $t = 0$, the first state corresponds to $t = 77130$, the second one to $t = 217530$ and the last one to $t = 553110$.

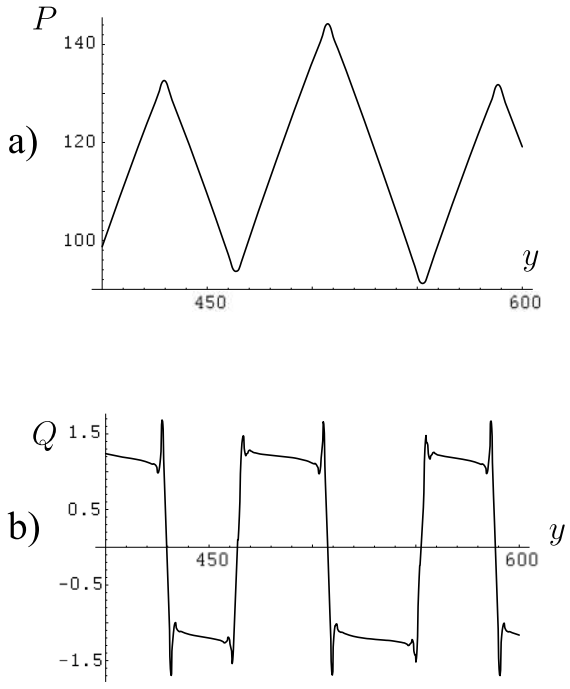

Fig. 5. Cubic spline of the: (a) interface position $P(y,t)$; and (b) its first derivative $Q(y,t) \equiv \partial P(y,t)/\partial y$ at given time.

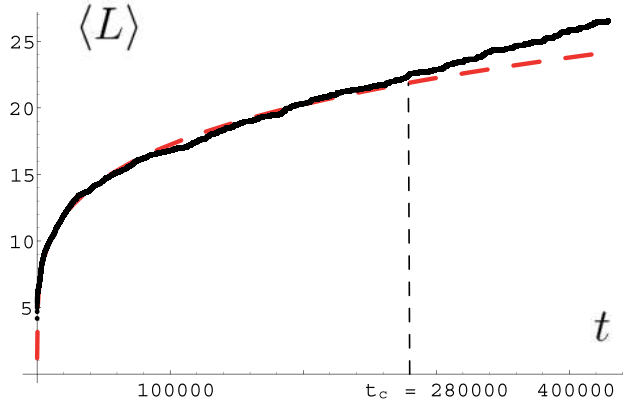

Fig. 6. Numerical computation of $\langle L \rangle(t)$ from the average of two simulations (solid line). A power law fitting $\langle L \rangle(t) \approx 1.19 t^{0.23}$ (dashed line).

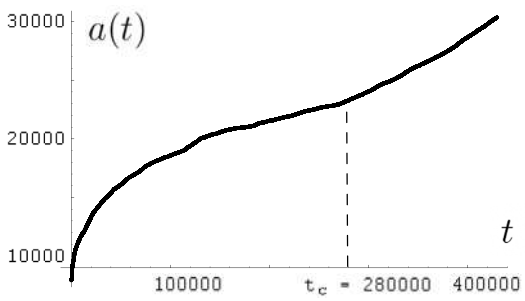

Fig. 7. Numerical computation of the area of the nonzero solution $|A_+|$ as function of time $a(t)$.

where $\lambda(k)$ is constant for a fixed k. This growth rate, or $\lambda(k)$-spectrum, is displayed in Fig. 3 as a function of the wavenumber k. The $\lambda(k)$-spectrum allows us to conclude that the front (2) is linearly unstable; its maximum corresponds to the characteristic wavenumber exhibited by the system during the development of the instability. The modes

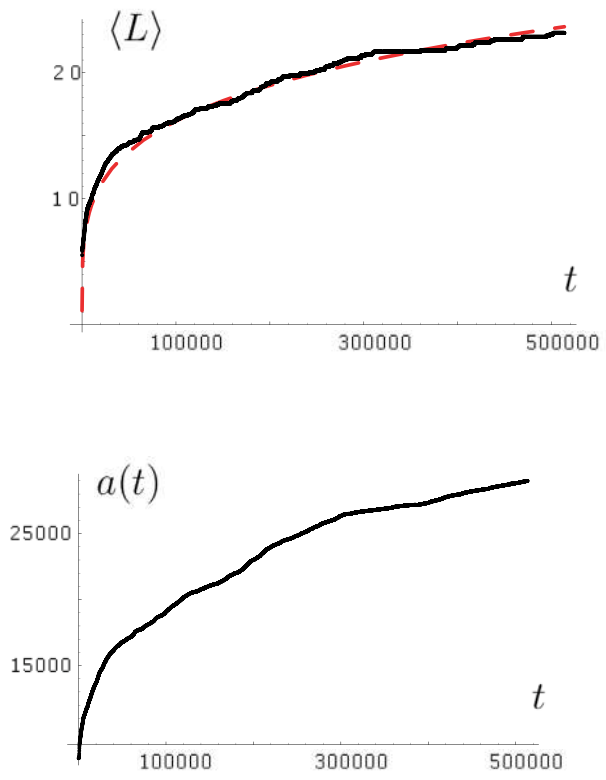

Fig. 8. Numerical computation of: (a) $\langle L\rangle(t)$ (solid line), and the power law fitting $\langle L\rangle(t) \approx 1.12t^{0.23}$ (dashed line); and (b) $a(t)$. For $y \in [0, 499]$.

with the shortest wavelength are stable, while the modes with the longest ones are unstable. Note that $\lambda(0) = 0$, as it is expected from the translational invariance.

The $\lambda(k)$-spectrum evokes us the classical Cahn–Hilliard equation spectrum [53,54], namely, $\lambda(k) \propto \alpha k^2 - k^4$. Since the modes with the longest wavelength are never stabilized, we expect that the characteristic length of the interface profile increases monotonically with time, i.e. developing a *coarsening* process, in a similar way to the Cahn–Hilliard model [54]. It is important to remark a difference with the Cahn–Hilliard equation spectrum: the $\lambda(k)$-spectrum, which is shown in Fig. 3, seems to be flat at small k.

4. Nonlinear regime: zigzag structure and coarsening dynamics

After the linear regime, the interface shows a zigzag structure (see Fig. 4). Namely, the interface is composed of line pieces with an apparently well-defined slope, zig-facet or zag-facet, turned with well-defined angles. Two adjacent facets, whose orientations are opposite, are connected by a region of strong curvature, that we term corner. Fig. 5 illustrates the interface position $P(y,t)$ and its first derivative $Q(y,t) \equiv \partial P(y,t)/\partial y$ at a given time, which corresponds to a cubic spline interpolation of data that comes from a direct numerical simulation of model (1). From the Q-shape it is possible to infer that the facets have approximatively the same slope, with opposite signs, plus a small curvature. This curvature is smaller when the domain size in some facets increases. At the corners, the behavior of Q is not monotonic, which is a reminiscence of convective effects in the Cahn–Hilliard equation [55]. In the convective Cahn–Hilliard model, the absence of monotonicity is observed only at the transition from a negative slope to a positive slope, due to adjusting of the system induced by the asymmetry of a single kink solution [56]. In our case, the non-monotonicity is observed in both transitions.

The dynamics shown by the interface consists then in reassembling domains of even orientation, i.e. a coarsening dynamics. This process occurs due to annihilations of corners (see the temporal sequence in Fig. 4) and without a characteristic length scale. Actually, the averaged size of the domain with a well defined slope increases regularly in time. Fig. 6 shows the measure of the temporal evolution of the averaged size of these domains, which we term $\langle L\rangle(t)$. It comes from the result of two numerical simulations with a different initial noisy perturbation. We compute $\langle L\rangle$ for both simulations each $\Delta t = 10$ time step. The solid line in Fig. 6 is the average of these two values of $\langle L\rangle$. Note that, for moderated time the averaged size seems to grow with the power law $\langle L\rangle \sim t^{0.23}$ (dashed line), later on (after $t_c \approx 2.8 \times 10^5$), $\langle L\rangle$ exhibits a change of its growing speed. Since, the non-monotonic behavior of Q, at the corners, evokes us the convective effect in the Cahn–Hilliard model, we expect to observe, even at the Maxwell point, some propagation of one uniform state over the other. In fact, in Fig. 7 we display the area of the nonzero solution (the amplitude of pattern $|A_+|$) as a function of time $a(t)$, from the same data that we used to compute $\langle L\rangle$, namely, a is the averaged area of two simulations. $a(t)$ increases monotonically on time, i.e. the stripes invades the uniform solution. Note that, after $t_c \approx 2.8\times10^5$ the propagation speed of the area also exhibits a qualitatively change of its dynamical behavior. Namely, after t_c the propagation speed increases, giving the impression that the zigzag interface is pushed.

Since the behavior exhibited by the interface seems to be similar to the faceting of a growing crystal surface modeled by the convective Cahn–Hilliard equation, one might expect to deduce a Cahn–Hilliard-like equation, in the form $\partial_t Q = F\left(Q, \partial_y Q, \partial_{yy} Q, \ldots\right)$. However, this is not possible. The reason becomes evident from Fig. 4: at the linear regime, the phase excitation takes place around the interface, i.e. at the region $x \sim P(y)$, however, this excitation begins to propagate far from the interface, due to the phase diffusion process undergone by the phase (see the review [2] for a discussion of phase diffusion in amplitude equations). Hence, the coarsening dynamic is always affected by processes that occur far from the interface, and it is not possible to reduce to an effective one-dimensional dynamics (the y-dimension), as it is necessary for the Cahn–Hilliard type approach [54].

Therefore, transversal variations at the interface play the role of a source of phase; the phase created by the source increases the transversal variations, i.e., the source of phase is amplified by the phase that it creates. Then, there is a *feedback interaction between phase and interface*, which is responsible for the observed dynamics. The created phase diffuses far from the interface; however, the diffusion in the transversal direction affects the coarsening at the interfaces. This explains the efficiency of the process, even for large $\langle L\rangle$, in contrast with the convective Cahn–Hilliard equation which has a logarithmic crossover for large time. In this sense, the coarsening process is non-local and is affected by the domain of the system. That is, it is not possible to make an effective one-dimension reduction of the dynamics around the interface.

The change exhibited by the growing speed of $\langle L\rangle$ at t_c, could be induced by the border of the system, even if the interface is far from the border, the phase excitation is close to it (see Fig. 4, lower panel, Im[A]). In order to verify this hypothesis, we have done numerical simulations increasing the transversal size of the system—we consider a transversal domain $0 \le y \le 499$. As we see in Fig. 8 no change in the growing speed of $\langle L\rangle$ or $a(t)$ is observed until $t = 5.1 \times 10^5$. This is a clear evidence that the existence of a t_c is a boundary effect.

Note that, the responsible of the interaction between phase and interface is the imaginary part of the Newell–Whitehead–Segel spatial operator

$$\mathrm{Im}\left[\left(\partial_x - i\partial_{yy}\right)^2\right] = -2\partial_{xyy},$$

which is related with the isotropy of the underlying pattern forming system. The amplitude Eq. (1) preserve the fact that stripes formation is a spontaneous breaking of the rotational symmetry. Therefore, the

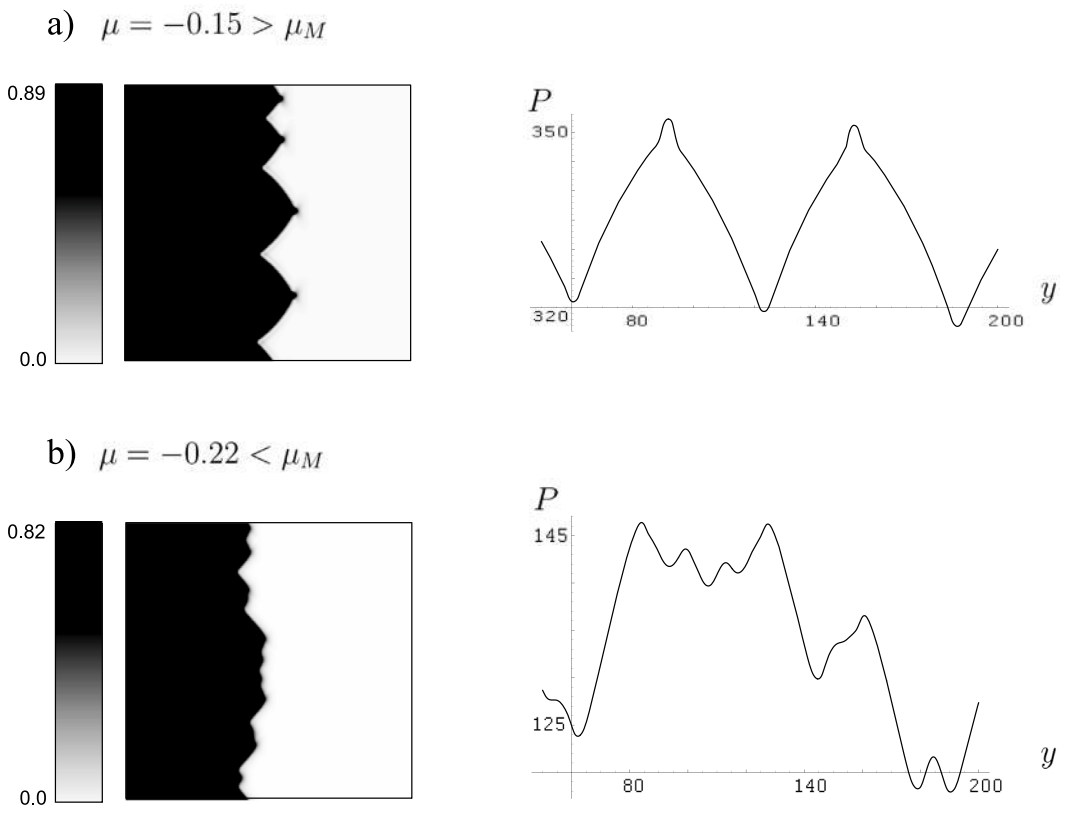

Fig. 9. Numerical simulations of model (1) for: (a) $\mu = -0.15$; and (b) $\mu = -0.22$. (left) A density plot of $|A|$ and (right) the transversal profile of the interface $P(y)$.

instability seems to be related to the isotropy of the underlying pattern-forming system, indeed, for a strong anisotropic system (where the stripes only can be formed in a privileged direction) this differential operator must be replaced by an isotropic (completely real) Laplace operator [57]. In this last case, one does not observe these kinds of transversal instabilities [58].

5. Phenomenology out of the Maxwell point

In the parameter space out of the Maxwell point $\mu \neq \mu_M = -3/16$, there is not a static domain wall that links the two uniform states. Due to the process of minimization of the Lyapunov potential of the model (1), one of the uniform states invades the other one. Then, the interface now has another propagation mechanism which is not related to the transversal deformation of the flat interface.

To analyze the transversal stability of these moving fronts, we performed the same numerical experiments that in the Maxwell point, with $\mu = -0.15 > \mu_M$ and $\mu = -0.22 < \mu_M$, in order to study the behavior of the interface when the-non zero uniform state is more stable than the zero amplitude state and vice-versa. Numerically we observe that in addition to the extra speed, the phenomenology is the same. That is, the flat interface is transversally unstable and the nonlinear regimen is characterized by a coarsening dynamics of a zigzag structure. The main phenomenological difference is in the shape of the zigzag structure. Fig. 9(a) depicts the front profile for $\mu = -0.15$, i.e when the uniform solution $A = A_+$ is energetically more convenient than $A = 0$ ($\mathcal{F}[A_+] < \mathcal{F}[0]$). In this case, the facets show a strong curvature, which is probably induced by the tendency of the system to propagate over the nonzero amplitude state. Analogously, we expect to observe the opposite behavior when $\mu = -0.22 < \mu_M$, however, in this case, the facets remain with a well-defined slope and the amplitude of the zigzag is lower than the one at the Maxwell point, as it is illustrated in Fig. 9(b).

6. Interface dynamics in subcritical-NWS versus subcritical Swift–Hohenberg equation

Since the amplitude Eq. (1) loses the pinning effect, a natural query is: What is the real meaning of these processes observed in subcritical-NWS in pattern-forming systems? To answer this question, we analyze a prototype mathematical model, the subcritical Swift–Hohenberg equation [6], which exhibits coexistence between a stable stripes pattern and a stable uniform state. This model reads

$$\partial_t u = \varepsilon u + \nu u^3 - u^5 - \left(\nabla^2 + q^2\right)^2 u, \tag{3}$$

where $u(x, y, t)$ is a real field (the order parameter), ε is the control parameter, q is the characteristic wavenumber of the pattern and ν is a parameter that controls the type of bifurcation, for positive (negative) ν the bifurcation is sub (super) critical. The uniform solution $u = 0$ becomes unstable when $\varepsilon > 0$, and the model (3) exhibits the formation of a stripes pattern. For $\nu > 0$ there is a range of the control parameter (with $\varepsilon < 0$) where the stripes pattern coexists with a stable uniform state. Inside this coexistence region, one observes locked or motionless fronts connecting the stripes pattern with the uniform state.

The model (3) can be approached by the amplitude Eq. (1) in the weakly nonlinear limit $\nu \sim \sqrt{|\varepsilon|} \ll 1$, keeping $q \sim \mathcal{O}(1)$. In this limit, one can approach the order parameter by

$$u \approx \sqrt{\frac{6\nu}{5}} \mathrm{Re}\left[A e^{iqx}\right] + \mathcal{O}\left(\nu^{5/2}\right),$$

where the amplitude A obeys Eq. (1), with $\mu \equiv 9\varepsilon/10\nu^2$, and introducing the slow spatiotemporal variables

$$\frac{9\nu^2 t}{10} \to t, \quad \frac{3\nu x}{2q\sqrt{10}} \to x \quad \text{and} \quad \sqrt{\frac{3\nu}{\sqrt{10}}} y \to y.$$

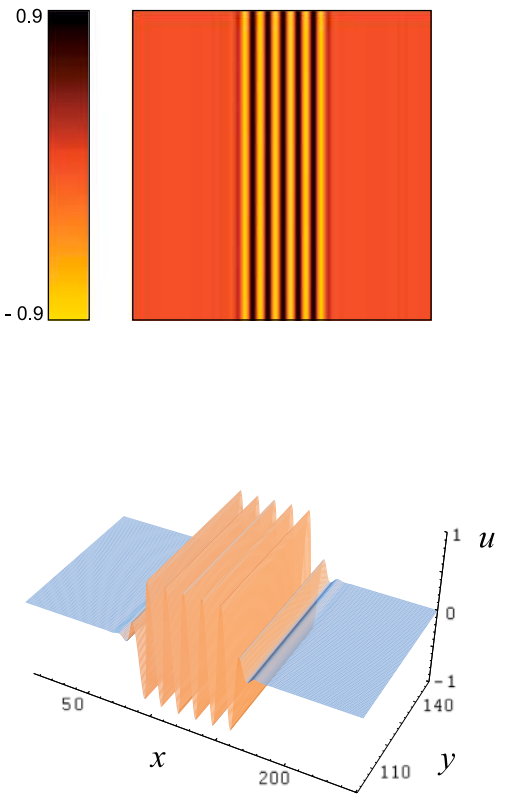

Fig. 10. Localized stripes from a direct numerical simulation of the model (3), for $\epsilon = -0.07$, $\nu = 0.7$ and $q = 0.5$. (upper panel) Density plot of the order parameter; (lower panel) a 3D plot of the same structure.

Here, we report numerical simulations of the model (3) using a pseudo-spectral method. Since, this numerical method demands periodical boundary conditions, to study the transversal stability of a flat interface between stripes and the uniform state, we considered as initial condition localized stripes. This solution is formed by two domain walls. In fact, fixing the parameters $q = 0.5$ and $\nu = 0.7$, we performed the following numerical simulations: we prepared localized structures from the one-dimensional version of model (3), and we extended it in the transversal dimension (y-direction); then, we added a small noisy perturbation and considered this configuration as initial condition of the model Eq. (3). We always observe that the system evolves back to the transversally flat configuration and remain at rest forever. These types of stable quasi-one-dimensional structures have been earlier observed in Ref. [59]. Fig. 10 shows a typical localized stripes pattern.

Hence, a flat front of prototype model (3) is transversally stable for these parameters, and does not develop the same instability that exhibits the amplitude Eq. (1). It is possible to claim that, the parameters chosen for the numerical analysis are far away to the weakly nonlinear limit. However, if we decrease ν, the system (3) displays another type of instability [29] (that we briefly comment below), which is not related to the zigzag structure that exhibits model (1). However, the above scenario changes drastically if we consider permanent stochastic fluctuations, i.e. noise. We have performed numerical simulations adding white noise to model (3), that is

$$\partial_t u = \epsilon u + \nu u^3 - u^5 - \left(\nabla^2 + q^2\right)^2 u + \sqrt{\eta}\xi\left(x,y,t\right), \tag{4}$$

where η is the noise intensity and $\xi\left(x,y,t\right)$ is a Gaussian white noise, with zero mean value $\langle\xi\left(x,y,t\right)\rangle = 0$ and correlation $\left\langle\xi\left(x,y,t\right)\xi\left(x',y',t'\right)\right\rangle = \delta\left(x-x'\right)\delta\left(y-y'\right)\delta\left(t-t'\right)$. This is a more accurate description because all macroscopic non-equilibrium systems represented by order parameter equations, like model Eq. (3), exhibit internal fluctuations such as thermal fluctuations [1].

Fig. 11 shows the result of a numerical simulation of the model (4), the initial condition corresponds to the stable localized structure shown in Fig. 10. Initially, the system exhibits a transversal spatial structure at the interfaces with a characteristic size that corresponds to half of the pattern wavelength. Later on, these spatial oscillations merge and nucleate new oscillations. When this process evolves the interfaces form a zigzag structure (cf. Fig. 11), which displays a coarsening dynamics, in a similar way to those exhibited by the amplitude Eq. (1). Subsequently, as the zigzag evolves, the pattern phase is clearly modified from the interface, as it is depicted in Fig. 11. Note that, the pattern is quickly propagating over the uniform state, then facets at the interface evolve a curvature for larger times. Hence, the dynamical behavior is more similar to the one observed in Eq. (1), for $\mu > \mu_M$ (see Fig. 9(a)), suggesting that the stripes pattern are energetically more convenient than the uniform state for the parameters chosen. For $\epsilon < -0.07$, inside the pinning range, the interface evolves initially in a similar manner, however, the coarsening dynamics evolves slowly and the system seems to be frozen in some zigzag profile.

In brief, a flat interface of the deterministic model (3) is linearly stable (at least for the parameters shown in Fig. 10), however in presence of noise the interface develops a transversal zigzag structure, which displays a coarsening dynamic. Then, a flat interface is nonlinear transversally unstable, in the sense that the system seems to be trapped in a metastable state. In presence of noise, the system is able to escape from this metastable state and develops a similar transversal instability to the amplitude Eq. (1). This scenario is pictorially depicted in Fig. 12. Furthermore, if this scenario is correct, then, a strong perturbation on the initial condition should trigger the instability. In fact, Fig. 13 displays this situation, where a spot is located in the right-wall. As a consequence of this non-small perturbation, the system starts to develop a corner from the position of the spot, trigging the depinning process. Note the strong distortion of the pattern phase, as well as the strong curvature of the facets.

Probably, the mechanism responsible to lock the transversal dynamics of the flat interface is closely related to the pinning effect observed in one-dimension systems. In fact, both phenomena are lost in the amplitude equations approach. This statement suggests that both phenomena come from the exponentially small corrections, which are neglected in the weakly nonlinear limit that is considered in the amplitude equation approach. Notice that a one-dimensional pinned interface, between a periodic state and a uniform one, is also a metastable state. In presence of noise one state starts to propagate over the other one [22,59], as in the two-dimensional case reported here (cf. Fig. 11). In one spatial dimension systems, the pinning effect can be understood in terms of the spontaneous breaking of the translational symmetry that implies the formation of the periodical pattern. Indeed, to propagate the cellular pattern or the uniform state, the system must nucleate or eliminate a pattern cell. That is, the front envelope should be moved a non-arbitrary finite length to pass to an equivalent state (a length that corresponds to half of the pattern wavelength, if the system has the reflection symmetry $u \to -u$). Hence, inside the pinning range, the interface should cross a nucleation barrier to propagate one state over the other one. In the two-dimensional case, shown in Fig. 11, it seems to be the same situation. In fact, the system initially leads to nucleate a spatially transversal structure at the interfaces whose characteristic size corresponds to half of the pattern wavelength. When the interface crosses the nucleation barrier, the pattern propagates to the uniform state. Since, in the weakly nonlinear regimen – where the amplitude Eq. (1) is deduced – the pattern wavelength is considered as a fast spatial scale, what is a finite wavelength for model (3), it is infinitesimal for Eq. (1). Therefore, the nucleation barrier is neglected in the amplitude equation approach. However, when the system crosses

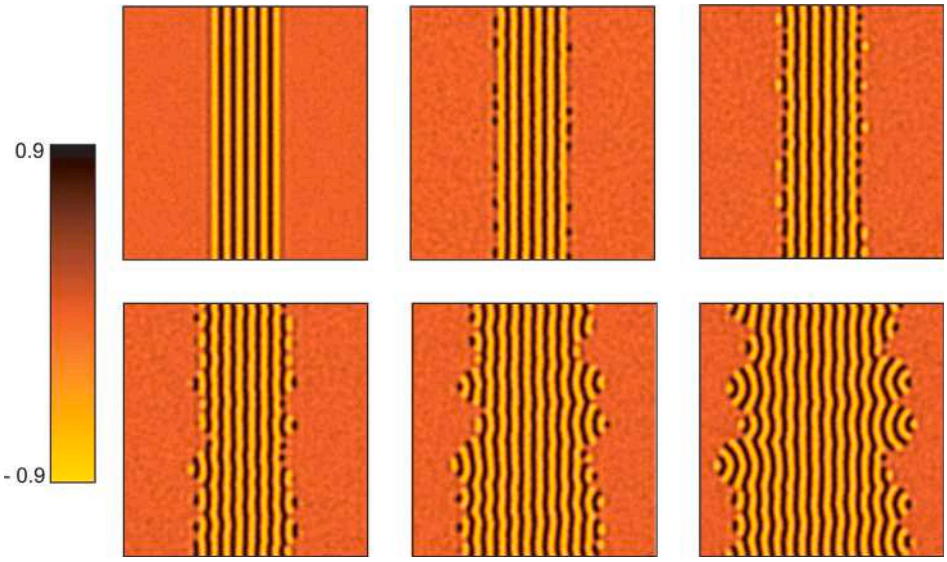

Fig. 11. Density plots of the order parameter from a numerical simulation of model (4), for $\varepsilon = -0.07$, $\nu = 0.7$, $q = 0.5$ and $\eta = 0.1$. Time grows from left to right, and up to down.

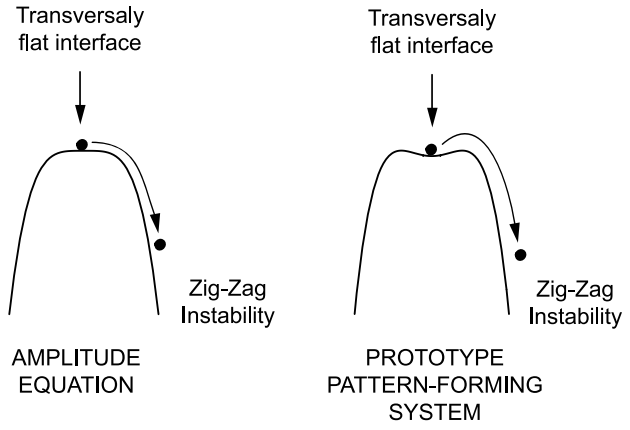

Fig. 12. Schematic representation of the transversal zigzag instability, in both scenarios: (left) the amplitude Eq. (1); and (right) the prototype pattern-forming system (3).

the nucleation barrier, then it exhibits a similar dynamics with the amplitude Eq. (1), that is, the zigzag dynamics.

Furthermore, as we mention above, decreasing ν the system displays another kind of transversal instability, that leads to the formation of a spatially periodic structure at the domain walls. The details about the formation of such structures can be found in Refs. [28–30], Fig. 14(a) shows one of them. Here, again, the configuration loses stability under the presence of fluctuations (see Fig. 14(b)), and the system displays the zigzag dynamics. Therefore, the robust dynamics, that this prototype pattern-forming system performs, is the process depicted by Eq. (1), and all the structures induced by the pinning effect are metastables.

The main ingredients of the prototype model (3) are: the formation of stripes patterns from a uniform state through a subcritical bifurcation, homogeneity, isotropy, and reflection symmetry ($u \to -u$). These are the only features necessary to deduce the amplitude Eq. (1), in the weakly non-linear regimen. Hence, we expect to observe a similar behavior – non-linear transversal zigzag instability – in different frameworks that exhibit the same spatial bifurcation and the same underlying symmetries.

7. Conclusions

The amplitude Eq. (1) models the spatiotemporal evolution of the envelope of stripes pattern, which emerges through a subcritical bifurcation, in a weakly nonlinear regime, where the underlying pattern-forming system is homogeneous and isotropic. Hence, the pattern formation is a spontaneous breaking of the rotational and the translational symmetries. Model (1) maintains the effect of breaking the rotational symmetry in the anisotropy of its differential operator. However, this model loses the information about the breaking of the translational symmetry, because in the weakly nonlinear regimen the pattern wavelength does not play any role. A flat interface that links the zero amplitude solution (uniform state of the original system) with the stable nonzero amplitude solution (pattern state of the original system) is transversally unstable. Then, after an infinitesimal perturbation, the flat interface initially develops a transversal structure with a well-defined wavelength. Later on, this transversal structure becomes a zigzag structure, which exhibits a coarsening dynamics.

The instability and the coarsening dynamics are consequences of the feedback interaction between the pattern phase and the interface position. Transversal variations of the interface induce excitation of the pattern phase, which induces transversal variations of the interface. So, the excitation of the pattern phase diffuses far from the interface; the coarsening process is an intrinsically non-local phenomenon.

The above picture changes if we study the same phenomena in a prototype model of pattern formation—the subcritical Swift–Hohenberg Eq. (3). As a consequence of the pinning effect, a transversally flat interface between stripes and a uniform state is stabilized. Since model (1) loses the information about the translational breaking symmetry, then this approach loses the pinning effect. However, in presence of noise, model (3) exhibits the same dynamical behaviors as those exhibited by the amplitude Eq. (1). So, the interface develops a transversal zigzag profile, which shows a coarsening dynamics. Therefore, in connection with our previous work [29], we are able to claim now that all these structures are transient (which, depending on the intensity of fluctuation, may have a long half-life), and the ultimate dynamics is the zigzag that we are documented in this report. The main features of the zigzag dynamics are contained in model (1). One of the main ingredients, to observe these processes, is the isotropy of the underlying pattern-forming system. Actually, for strong anisotropic systems, one

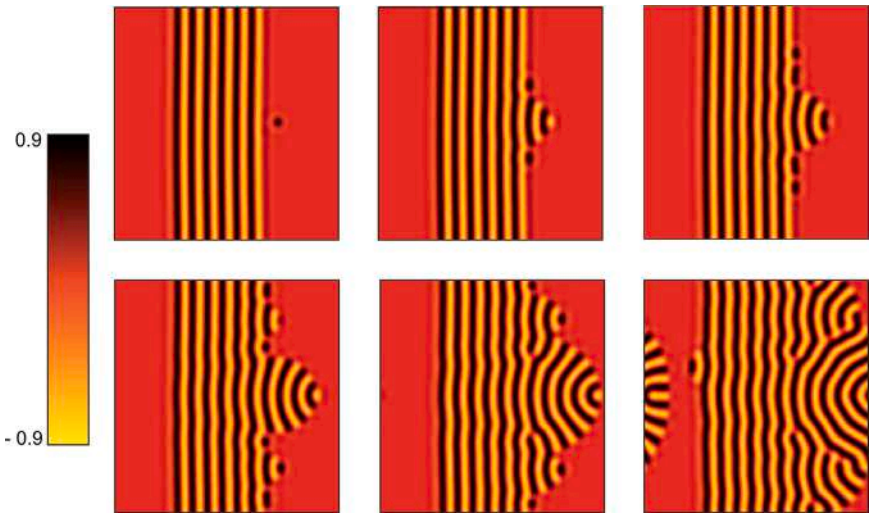

Fig. 13. Density plots of the order parameter from a numerical simulation of model (3), for $\varepsilon = -0.07$, $\nu = 0.7$ and $q = 0.5$. Time grows from left to right, and up to down.

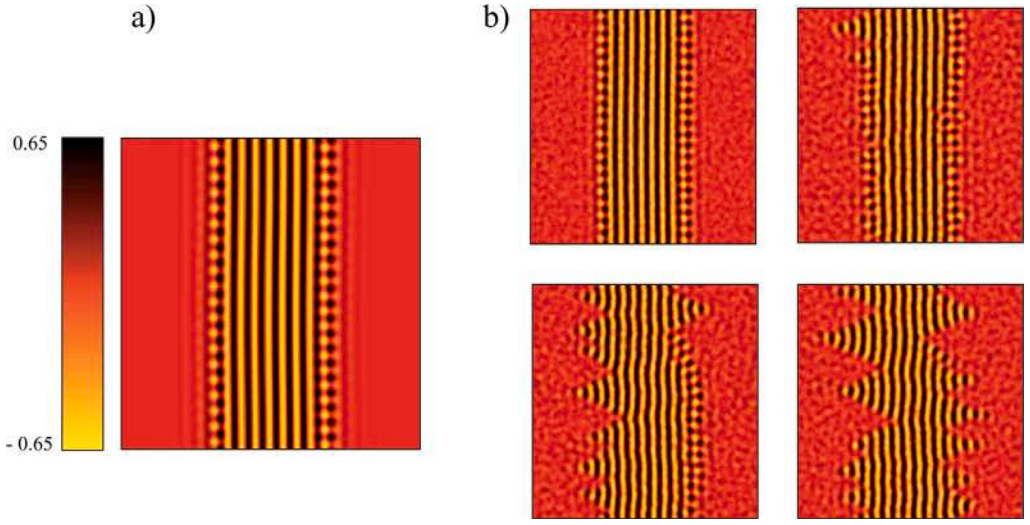

Fig. 14. Density plots of the order parameter from numerical simulations of: (a) model (3), for $\varepsilon = -0.0417$, $\nu = 0.5$ and $q = 0.7$. (b) model (4), for $\varepsilon = -0.0417$, $\nu = 0.5$, $q = 0.7$ and $\eta = 0.07$, time grows from left to right, and up to down.

can have other kind of behaviors [58], which are not related to the zigzag reported here. Due to ubiquitous of the stochastic fluctuations in nature, we expect that the transversal structures described in this work are robust. Furthermore, the zigzag dynamics might be also triggered by an irregular initial condition.

CRediT authorship contribution statement

Marcel G. Clerc: Participated in the original discussion of the problem and in the paper writing. **Daniel Escaff:** Made the original calculations (both, analytical and numerical calculations), and wrote the first draft of the paper. **René G. Rojas:** Improved many of the numerical results that we are presenting in this paper.

Declaration of competing interest

The authors declare the following financial interests/personal relationships which may be considered as potential competing interests: Daniel Escaff reports financial support was provided by Fondecyt (project 1211251). Marcel G. Clerc reports financial support was provided by ANID- Millenium Science Initiative Program-ICN17 012 (MIRO) and FONDECYT Project No. 1210353.

Data availability

No data was used for the research described in the article.

Acknowledgments

D. E. thanks the financial support of Fondecyt, Chile project 1211251. MGC thanks for the financial support of ANID-Millenium Science Initiative Program, Chile-ICN17_012 (MIRO) and FONDECYT, Chile Project No. 1210353.

References

[1] Nicolis G, Prigogine I. Self-organisation in non equilibrium systems. In: From dissipative structures to order through fluctuations. New York: J.Wiley & sons; 1977.
[2] Cross MC, Hohenberg PC. Rev Modern Phys 1993;65:851.
[3] Aranson IS, Tsimring LS. Rev Modern Phys 2006;78:641.
[4] Capasso Vincenzo, Gromov Misha, Harel-Bellan Annick, Morozova Nadya, Pritchard Linda Louise. Pattern formation in morphogenesis: Problems and mathematical issues. In: Springer proceedings in mathematics book, vol. 15. 2012.
[5] Clerc M, Tlidi M. Nonlinear dynamics: materials, theory and experiments. Springer; 2016.

[6] M.I. Rabinovich, Ezersky AB, Weidman PD. The dynamics of patterns. Singapore: World Scientific; 2000.
[7] Pismen LM. Patterns and interfaces in dissipative dynamics. Berlin: Springer; 2006.
[8] Newell AC, Whitehead JA. J Fluid Mech 1969;38:279.
[9] Fisher RA. Ann Eugen 1937;7:335;
Kolmogorov A, Petrovsky I, Piskunov. Bull. Univ. Moskou Ser. Int. Se. 1937;7(6):1.
[10] Murray JD. Mathematical biology. Berlin: Springer-Verlag; 1993.
[11] Kife P. Mathematical aspects of reacting and diffusing system. In: Levin S, editor. Lecture notes in biomathematics, vol. 28. New-York: Springer-Verlag; 1979.
[12] Manneville P. Dissipative structures and weak turbulence. San Diego: Academic Press; 1990.
[13] Odent V, Clerc MG, Falcon C, Bortolozzo U, Louvergneaux E, Residori S. Opt Lett 2014;39:1861.
[14] Alfaro-Bittner K, Castillo-Pinto C, Clerc MG, Gonzalez-Cortes G, Rojas RG, Wilson M. Phys Rev E 2018;98:050201, (R).
[15] Clerc MG, González-Cortés G, Morel MJ, Hidalgo PI, Vergara J. Phys Rev E 2022;105:054701.
[16] Clerc MG, Nagaya T, Petrossian A, Riera C, Residori S. Eur Phys J D 2004;28:435, Physica D. 199 149.
[17] Aronson DG, Weinberger HF. Adv Math 1978;30:33.
[18] Pomeau Y. Physica D 1986;23:3.
[19] Tlidi M, Mandel Paul, Lefever R. Phys Rev Lett 1994;73:640.
[20] Scroggie AJ, Firth WJ, Mcdonald GS, Tlidi M, Lefever R, Lugiato LA. Chaos Solitons Fractals 1994;4:1323.
[21] Tlidi M, Mandel Paul. Chaos Solitons Fractals 1994;4:1475.
[22] Aranson IS, Malomed BA, Pismen LM, Tsimring LS. Phys Rev E 2000;62:R5;
Clerc MG, Falcon C, Tirapegui. E. Phys. Rev. Lett. 2005;94:148302.
[23] Haudin F, Elías RG, Rojas RG, Bortolozzo U, Clerc MG, Residori S. Phys Rev Lett 2009;103:128003.
[24] B.A. Malomed, Nepomnyashchy AA, Tribelsky MI. Phys Rev A 1990;42:7244.
[25] Clerc MG, Falcon C. Physica A 2005;356:48.
[26] Bortolozzo U, M.G. Clerc, Falcon C, Residori S, Rojas R. Phys Rev Lett 2006;96:214501.
[27] Hagberg A, Yochelis A, Yizhaq H, Elphick C, Pismen L, Meron E. Physica D 2006;217:186.
[28] Burke J, Knobloch E. Chaos 2007;17:037102.
[29] M.G. Clerc, Escaff D, Rojas R. Europhys Lett 2008;83:28002.
[30] Avitabile Daniele, Lloyd David JB, Burke John, Knobloch Edgar, Sandste Bjorn. Siam J Appl Dyn Syst 2010;9(3):704–33.
[31] Coelho Daniel L, Vitral Eduardo, Pontes José, Mangiavacchi Norberto. Physica D 2021;427:133000.
[32] Berrios-Caro E, Clerc MG, Ferre MA, Leon AO. Phys Rev E 2018;97:012207.
[33] Umbanhowar a Paul B, Melo b Francisco, Swinney Harry L. Physica A 1998;249:1–9.
[34] Segalman Rachel A. Mater Sci Eng R 2005;48:191–226.
[35] Gonzalez-Lakunza N, Fernandez-Torrente I, Franke KJ, Lorente N, Arnau A, Pascual JI. Phys Rev Lett 2008;100:156805.
[36] Fernandez-Torrente I, Kreikemeyer-Lorenzo D, Strozecka A, Franke KJ, Pascual JI. Phys Rev Lett 2012;108:036801.
[37] Alonso A, Batiste O, Knobloch E, Mercader I. Convectons. In: Descalzi O, Clerc M, Residori S, Assanto G, editors. Localized states in physics: solitons and patterns. Berlin, Heidelberg: Springer; 2011, http://dx.doi.org/10.1007/978-3-642-16549-86.
[38] Jacono David Lo, Bergeon Alain, Knobloch Edgar. J Fluid Mech 2011;687:595–605.
[39] Beaume Cédric, Bergeon Alain, Knobloch Edgar. J Fluid Mech 2018;840:74–105.
[40] Bordeu Ignacio, Clerc Marcel G, Couteron Piere, Lefever René, Tlidi Mustapha. Sci Rep 2016;6(1):1–11.
[41] Tlidi Mustapha, Bordeu Ignacio, Clerc Marcel G, Escaff Daniel. Ecol Indic 2018;94:534.
[42] Clerc MG, Esca? D, Kenkre VM. Phys Rev E 2005;72:056217.
[43] Clerc MG, Esca? D, Kenkre VM. Phys Rev E 2010;82:036210.
[44] Escaff D. Int J Bifurcation Chaos 2009;19:3509.
[45] Escaff D. Eur Phys J D 2011;62:3338.
[46] Fernandez-Oto C, Clerc MG, Escaff D, Tlidi M. Phys Rev Lett 2013;110:174101.
[47] Fernandez-Oto C, Tlidi M, Escaff D, Clerc MG. Phil Trans R Soc A 2014;372:20140009.
[48] Escaff D, Fernandez-Oto C, Clerc3 MG, Tlidi M. Phys Rev E 2015;91:022924.
[49] Odent V, Tlidi M, Clerc MG, Glorieux P, Louvergneaux E. Phys Rev A 2014;90:011806, (R).
[50] Peschel U, Michaelis D, Etrich C, Lederer F. Phys Rev E 1998;58:R2745.
[51] Tlidi M, Vladimirov2 AG, Mandel Paul. Phys Rev Lett 2002;89:233901.
[52] Andrade-Silva Ignacio, Clerc Marcel G, Gonzalez-Cortes Gregorio, Vincent Odent PR. Research 2021;3:L022027.
[53] Cahn JW, Hilliard JE. J Chem Phys 1958;28:258.
[54] Calisto H, Clerc MG, Rojas R, Tirapegui E. Phys Rev Lett 2000;85:3805;
Argentina M, Clerc MG, Rojas R, Tirapegui E. Phys. Rev. E 2005;71:046210.
[55] Golovin AA, Nepomnyashchy AA, Davis SH, Zaks MA. Phys Rev Lett 2001;86:1550.
[56] Waston SJ, Otto F, Rubinstein Y, Davis SH. Physica D 2003;178:127;
Podolny A, Zaks MA, Rubinstein BY, Golovin AA, Nepomnyashchy AA. Physica D. 2005;201:291.
[57] Weber A, Bodenschatz E, Kramer L. Adv Mater 1991;3:191.
[58] Clerc MG, Falcon C, Escaff D, Tirapegui E. Eur. Phys. J. Spec. Top. 2007;143:171.
[59] Sakaguchi H, Br H. Physica D 1996;97:274.